AGU PUBLICATIONS

JGR

Journal of Geophysical Research: Space Physics

RESEARCH ARTICLE

10.1002/2015JA021749

Key Points:
- We proposed a new method to identify larger-amplitude interplanetary Alfven wave
- The new method is independent of the HT frame and background magnetic field and works well
- Wave property in frequency domain is obtained for Alfven waves

Correspondence to:
H. Li and C. Wang,
hli@spaceweather.ac.cn;
cw@spaceweather.ac.cn

Citation:
Li, H., C. Wang, J. K. Chao, and W. C. Hsieh (2016), A new approach to identify interplanetary Alfvén waves and to obtain their frequency properties, *J. Geophys. Res. Space Physics*, *121*, 42–55, doi:10.1002/2015JA021749.

Received 31 JUL 2015
Accepted 24 DEC 2015
Accepted article online 29 DEC 2015
Published online 21 JAN 2016

A new approach to identify interplanetary Alfvén waves and to obtain their frequency properties

H. Li[1], C. Wang[1], J. K. Chao[2], and W. C. Hsieh[2]

[1]State Key Laboratory of Space Weather, Center for Space Science and Applied Research, Chinese Academy of Sciences, Beijing, China, [2]Institute of Space Science, National Central University, Taoyuan, Taiwan

Abstract Conventional diagnosis of interplanetary Alfvén waves requires an accurately determined de Hoffmann-Teller (HT) frame or background magnetic field. For simplicity, the averaged HT frame and the mean value of the magnetic field are often used in the literature. However, HT frame can change quite fast in high-speed solar wind streams, and it is not always appropriate to take the average value of the magnetic field to be the background state. In order to reduce the uncertainty introduced by determining HT frame and background magnetic field, we propose a new approach for identifying large-amplitude interplanetary Alfvén waves. This new approach is independent of HT frame and of background magnetic field. Instead of the original data sets, the band-pass filtered signals of plasma velocity and magnetic field observations are used to check the Walén relation. The robustness of this technique is verified by applying to simulated pure Alfvén waves with two separate frequencies and contaminated by pink colored noises in a varying solar wind stream. Furthermore, in our approach, more properties of Alfvén waves in frequency domain can be obtained, which have been rarely discussed before. Our analysis technique is applied to two intervals of solar wind high-speed streams, and it is shown that large-amplitude Alfvén waves near 1 AU are frequently found during these two intervals.

1. Introduction

Alfvén [1942] first suggested the existence of electromagnetic-hydromagnetic waves in 1942. As a type of magnetohydrodynamic wave, an Alfvén wave in a plasma is a low-frequency (compared to the ion cyclotron frequency) traveling oscillation of ions and magnetic field. The motion of the ions and the perturbation of the magnetic field are in the same/opposite direction and transverse to the propagating direction. Compared to magnetoacoustic wave modes, Alfvén waves are only slightly damped. Thus, most of the energy of fluctuations in the solar wind, especially in high-speed streams, has a clear Alfvénic nature [*Bruno et al.*, 2006].

In general, the study of the solar wind fluctuations can be classified into two main aspects: a turbulence description suggested by *Coleman* [1968] and an Alfvén wave description by *Belcher and Davis* [1971]. Both languages still face notable difficulties in explaining the related observations. On the one hand, the wave description could not interpret why the power law spectrum of the magnetic field fluctuations still obeys Kolmogorov's power law, which was derived for isotropic fluid turbulence [*Coleman*, 1968; *Dobrowolny et al.*, 1980; *Wang et al.*, 2012]. Kinetic Alfvén waves interact nonlinearly with each other and form a power law turbulent spectrum. On the other hand, the turbulence description is unable to account for well-ordered wave structures observed on different temporal scales [*Riley et al.*, 1996] and for no direct interactions between outward propagating Alfvén waves in different directions. Thus, a linear superposition of Alfvén waves and convective magnetic structures (like 2-D turbulence) was proposed to reconcile these two descriptions [e.g., *Matthaeus et al.*, 1990; *Tu and Marsch*, 1993]. For simplicity and conceptual clarity, the wave description is used to discuss the microscale solar wind fluctuations in this work.

Large-amplitude Alfvén wave (typically, the relative magnetic field fluctuation is comparable to or larger than 1) is a fundamental physical phenomenon in all kinds of magnetized plasmas. It contributes to a variety of physical processes in space plasmas, e.g., solar corona heating [e.g., *Wentzel*, 1974; *McIntosh et al.*, 2011], solar wind acceleration [e.g., *Alazraki and Couturie*, 1971; *McIntosh et al.*, 2011], and generation of geomagnetic disturbances [*Tsurutani and Gonzalez*, 1987]. Therefore, Alfvén waves are perhaps the most intriguing wave mode and have attracted a great deal of interest in space physics.

In situ measurements of the solar wind in the ecliptic plane have shown that interplanetary large-amplitude Alfvén waves are frequently found at the trailing edge of high-speed solar wind streams originating from solar coronal holes and after the corotating interaction regions. And the time period of such microscale fluctuations varies from several minutes to a few hours [*Belcher and Davis*, 1971; *Bruno et al.*, 1985; *Mavromichalaki et al.*, 1988]. *Coleman* [1967] first found some Alfvénic-like large-amplitude fluctuations in the data measured by Mariner 2 during its flight to Venus in the interplanetary medium. Later then, *Unti and Neugebauer* [1968], *Belcher et al.* [1969], and *Belcher and Davis* [1971] confirmed the good correlations between the fluctuations of observed magnetic field **B** and velocity **V** and certified these fluctuations to be outward propagating Alfvén waves originating near or at the Sun.

According to ideal magnetohydrodynamics theory, interplanetary Alfvén waves are often characterized by constant plasma density, temperature and magnetic field magnitude, and by correlated fluctuations of velocity and magnetic field that are perpendicular to both the background magnetic field $\mathbf{B}_0$ and wave vector $\mathbf{k}$ [*Walén*, 1944; *Belcher et al.*, 1969; *Hudson*, 1971; *Barnes and Hollweg*, 1974]. The two fluctuations are connected by the so-called Walén relation expressed in the form as follows:

$$\mathbf{V}_\perp = \pm\xi^{1/2}\frac{\mathbf{B}_\perp}{(\mu_0\rho)^{1/2}} + \text{const} \tag{1}$$

where $\mathbf{V}_\perp$ $(= \mathbf{V} - \mathbf{V}\cdot\hat{e}_{B_0})$ represents the plasma velocity fluctuation perpendicular to $\mathbf{B}_0$, and $\mathbf{B}_\perp$ $(= \mathbf{B} - \mathbf{B}\cdot\hat{e}_{B_0})$ represents the magnetic field fluctuation perpendicular to $\mathbf{B}_0$. $\hat{e}_{B_0}$ is the unit vector of $\mathbf{B}_0$. μ_0 is the permeability in vacuum, and ρ is the plasma mass density. The sign $\pm$ represents different propagation directions, parallel $(-)$ and antiparallel $(+)$ to $\mathbf{B}_0$. ξ is the thermal anisotropic parameter, which is given by

$$\xi = 1 - \mu_0\frac{P_\parallel - P_\perp}{B^2} \tag{2}$$

where $P_\parallel$ and $P_\perp$ are the thermal pressure parallel and perpendicular to the background magnetic field, respectively. In the solar wind near 1 AU (astronomical unit, the average distance from the Sun to the Earth), the thermal anisotropy is nonsignificant, and ξ is often assumed to be 1 [*Burlaga*, 1971a].

Sharply crested Alfvén waves are usually called Rotational Discontinuities (RDs). The above Walén relation for RD diagnosis in the spacecraft frame can be rewritten as

$$\Delta\mathbf{V} = \pm\Delta\mathbf{V}_\mathrm{A} \tag{3}$$

where the positive/negative sign applies if the normal components of the magnetic field and plasma velocity have the same/opposite signs. The symbol Δ represents the changes relative to the upstream state, for example, and $\mathbf{V}_\mathrm{A}$ is the local Alfvén velocity, corrected for the effect of pressure anisotropy,

$$\mathbf{V}_\mathrm{A} = \xi^{1/2}\frac{\mathbf{B}}{(\mu_0\rho)^{1/2}} \tag{4}$$

To evaluate the changes in equation (3) requires selection of the times between which the jumps are to be computed. Such choice is not necessary when performing the test in the de Hoffmann-Teller (HT) frame, in which frame the convective electric field vanishes in a uniform medium, and the flow velocity should be aligned parallel or antiparallel to the magnetic field [*de Hoffmann and Teller*, 1950]. In the HT frame, the Walén relation has a much simpler formulation and reduces to

$$\mathbf{V}' = \pm\mathbf{V}_\mathrm{A} \tag{5}$$

where $\mathbf{V}'$ $(= \mathbf{V} - \mathbf{V}_\mathrm{HT})$ is the plasma velocity in the HT frame.

The quantitative test of how well the Walén relation is satisfied is the so-called Walén test. The three forms of Walén relations given above are often used to classify Alfvén waves in interplanetary space [*Belcher et al.*, 1969; *Belcher and Davis*, 1971; *Neugebauer et al.*, 1984; *Scudder et al.*, 1999; *Neugebauer*, 2006; *Gosling et al.*, 2011; *Wang et al.*, 2012; *Paschmann et al.*, 2013; *Chao et al.*, 2014]. In general, the better the Walén relation is satisfied, the more pure Alfvénic in nature are the fluctuations. The solar wind Alfvénicity is defined to describe to what extent the fluctuations are purely Alfvénic and has been measured by several different parameters in the literature, such as the Alfvén ratio ($\gamma_\mathrm{A} =< \mathbf{v}^2 > / < \mathbf{b}^2 >$, $\mathbf{v}$ is the fluctuating velocity vector, $\mathbf{b}$ is the fluctuating magnetic field vector in Alfvén units, and brackets indicate averaging on the time domain), the Walén slope (slope of the regression line of the fluctuations of plasma velocity and magnetic field), the normalized cross helicity ($\sigma_C = 2 < \mathbf{v} \cdot \mathbf{b} > /(< \mathbf{v}^2 > + < \mathbf{b}^2 >)$), the normalized residual energy ($\sigma_R = (< \mathbf{v}^2 > - < \mathbf{b}^2 >)/(< \mathbf{v}^2 > + < \mathbf{b}^2 >)$), and the velocity-magnetic field correlation coefficient [*Belcher et al.*, 1969; *Neugebauer et al.*, 1984; *Bavassano et al.*, 1998; *Bruno et al.*, 2007; *Neugebauer*, 2006; *Gosling et al.*, 2011; *Paschmann et al.*, 2013; *Chao et al.*, 2014]. The case of either parameter is closer to 1; the fluctuation is more Alfvénic.

Previous studies reveal that the Alfvénicity decreases with increasing heliocentric distance from the Sun [e.g., *Tu and Marsch*, 1993; *Bavassano et al.*, 1998; *Neugebauer*, 2004]. For example, the Alfvénicity is found to be close to 1 near 0.3 AU [e.g., *Tu et al.*, 1990; *Marsch and Tu*, 1990]; however, most of the previous studies usually reported that the Alfvénicity is much less than 1 near 1 AU, of only 0.7 or less (see *Tu and Marsch* [1995] for a review). *Bruno et al.* [2007] provided a rough estimate of the importance of magnetically dominated structures (lower values of Alfvénicity) in the solar wind fluctuations and found a clear radial dependence of these magnetic structures within fast wind, but not within slow wind. At short heliocentric distances (~0.3 AU), the turbulent population was largely dominated by Alfvénic fluctuations; however, as the solar wind expands, magnetically dominated structures became visible. *Wang et al.* [2012] presented a clear case of pure large-amplitude Alfvén wave in the high-speed solar wind stream near 1 AU, with the Alfvénicity nearly equal to 1. They further suggested that such a purely Alfvénic fluctuation event rarely occurs at 1 AU.

To do the Walén test by using equation (1), an accurately determined background magnetic field is required. But the background magnetic field is not an observable quantity [*Lichtenstein and Sonett*, 1979; *Riley et al.*, 1996] or easily determined [*Gosling et al.*, 2010], and the mean value of the magnetic field is usually regarded as a proxy [see *Yang and Chao*, 2013, and the references therein]. It is not always appropriate to take the average value of the magnetic field to be the background state. *Riley et al.* [1996] deduced that the averaged magnetic field can be nearly perpendicular to the background state under certain model assumptions. *Gosling et al.* [2009] also showed that the solar wind fluctuations are relative to a slowing varying base value rather than to an average value and suggested that the conclusions derived from the analyses by assuming the fluctuations in all field components are relative to average values need to be reexamined. Equation (3) is more suitable for the diagnosis of RDs, which are sharply steepened Alfvén waves. Moreover, the selection of the times between which the jumps are to be computed is needed and could introduce some uncertainties. Recently, equation (5) is often used to do the Walén test. To use equation (5), the first important process is to accurately determine the HT frame. The existence of a HT frame requires a coherent quasi-stationary pattern of magnetic field and plasma velocity structure viewed in that frame. The observed temporal variations of such events are assumed to caused by the steady motion of the pattern relative to the instrument frame. However, the interplanetary medium is nonuniform and occupied by many dynamic structures with different size and duration, such as the magnetic flux ropes or tubes and discontinuities. In particular, the HT frame for a strictly perpendicular shock and a tangential discontinuity cannot be obtained. During the commonly used 1 h time interval, there may exist many dynamic structures. The HT frames for such structures may be significant different. In addition, even for a coherent quasi-stationary interplanetary structure, it is possible that its motion may be nonsteady. Thus, such an averaged HT frame derived from hourly observations may not be adequate. *Gosling et al.* [2009] and *Chao et al.* [2014] proposed a method which is independent of HT frame to check the Walén relation and which can predict Alfvénic fluctuations well. *Chao et al.* [2014] suspected that pure Alfvénic waves should be found frequently near 1 AU.

So far, numerous studies on interplanetary large-amplitude Alfvén waves have been done in the literature from both theoretical and observational aspects [see *Burlaga*, 1971b; *Völk*, 1975; *Yang and Chao*, 2013; *Bruno and Carbone*, 2013; *He et al.*, 2015, and the references therein]. Some aspects of the properties of Alfvén waves in the solar wind have been obtained, such as the origin, propagation, evolution, wave interval, Alfvénicity, generation mechanism, and other related properties [see *Yang and Chao*, 2013, and the references therein]. However, very little attention has been paid to their frequency properties. *Podesta and Borovsky* [2010] and *Podesta and Bhattacharjee* [2010] both showed that the normalized cross helicity of Alfvén waves was approximately constant throughout the inertial time scale, independent of wave number. *Wicks et al.* [2013] later investigated the effect of the joint distribution of the local normalized cross helicity and residual energy on the time scaling of the structure functions of the fluctuating fields. Meanwhile, because of the simplified preprocesses before the Walén test done by the previous studies, some statistical properties of Alfvén waves may need to be reexamined.

In this study, we are inspired to focus our attentions on the following aspects: (1) finding an approach which can remove/mitigate the effect of a varying HT frame or background magnetic field on the Walén test;

(2) obtaining the properties of Alfvén wave in frequency domain; and (3) checking whether interplanetary large-amplitude Alfvén wave can be found near 1 AU or not. The paper is organized as follows. The methodology and data set are described in section 2, the results are presented in section 3, the robustness verification is given in section 5, and the summary is given in section 5.

2. Methodology and Date Sets

The interplanetary magnetic field and solar wind plasma data in geocentric solar ecliptic (GSE) coordinates from the Wind spacecraft with a temporal resolution of 3 s [*Lepping et al.*, 1995; *Lin et al.*, 1995] are used to analyze the Alfvénic fluctuations. The contribution of the helium observation has been considered to evaluate the mass density (ρ) and velocity ($\mathbf{V}$) of the solar wind. Two intervals of solar wind high-speed streams are selected for our analysis: (1) 25 January to 10 February 1995 and (2) 11 to 28 October 2002. These two intervals are the same as that chosen by *Chao et al.* [2014].

As mentioned before, conventional analysis of Alfvén waves requires an accurately determined HT frame or background magnetic field to check the validity of the Walén relation. For simplicity, the HT frame velocity ($\mathbf{V}_{\rm HT}$) is often assumed to be stable during a concerned time interval and obtained from the minimum variance analysis (MVA) [*Sonnerup and Cahill*, 1967]. The methods of searching for the HT frame have been reviewed by *Chao et al.* [2014]. However, such an averaged HT frame may not be adequate sometimes, for example, when the solar wind contains many dynamic structures. Meanwhile, the MVA technique depends on the data points sampled. Sometimes, the result is quite sensitive to the time period concerned, and the relative difference is unacceptable. To avoid such problems, *Gosling et al.* [2009] and *Chao et al.* [2014] proposed a method using a sequence of data generated by taking the difference of two consecutive values of plasma and Alfvén velocities, which is independent of the HT frame.

We here will present a new approach to check the Walén relation by using the band-pass filtered signals of plasma velocity and magnetic field observations, instead of using the original data sets. At heliocentric distance beyond 0.3 AU, the power spectrum of the solar wind magnetic fluctuations are dominated by low-frequency (1 mHz ~ 0.1 Hz) Alfvén waves. For practice, we evenly divide this logarithmic frequency band into 10 parts. Thus, the periods of the filters are given as follows:

$$T_i = 10^{1+0.2*i} \quad (i = 0, 1, 2, 3, 4, \ldots) \tag{6}$$

The lower period T_0 is 10 s, which satisfies the Nyquist sampling theorem. The wave frequency is below the ion cyclotron frequency. The upper period is less than one third of the time interval of the data set, which ensures that the data set contain more than three complete wave cycles. Taking hourly data sets, for example, the filters are 10 s–15 s, 15 s–25 s, 25 s–40 s, 40 s–60 s, 60 s–100 s, 100 s–160 s, 160 s–250 s, 250 s–400 s, 400 s–630 s, and 630 s–1000 s. This approach can effectively reduce the influences of high-frequency measure uncertainties and low-frequency varying background fields (including the effect of spacecraft velocity). Usually, the unstable HT frame varies at a low frequency. This approach can remove the uncertainty introduced by a varying HT frame. Even if the varying frequency of the HT frame belongs to one of the band-pass filters, this will not affect the analysis of data sets with other filters. Furthermore, the property of pure Alfvén waves in the frequency domain can be obtained as well by checking the Walén relation for each band-passed signal as follows:

$$\delta \mathbf{V}_i = \pm \delta \mathbf{V}_{\rm Ai} \tag{7}$$

Here $\delta \mathbf{V}_i$ is the band-passed $\mathbf{V}$ with the ith filter. $\delta \mathbf{V}_{\rm Ai}$ is the band-passed $\mathbf{V}_{\rm A}$ with the ith filter.

Chao et al. [2014] suggested that the ratio of the standard deviations together with the correlation coefficient between plasma velocity fluctuation and Alfvén velocity fluctuation are better parameters for the Walén test. From their inspiration, a new parameter $E_{\rm rr}$ is defined to quantitatively assess the goodness of the Walén test or the Alfvénicity, as follows:

$$E_{\rm rr} = \text{average}\left[\left| |\gamma_c| - 1 \right|, \left| |\gamma_{ci}| - 1 \right|, \left| \frac{\sigma_{\delta \mathbf{V}}}{\sigma_{\delta \mathbf{V}_{\rm A}}} - 1 \right|, \left| \frac{\sigma_{\delta V_i}}{\sigma_{\delta V_{\rm Ai}}} - 1 \right| \right] \quad (i = x, y, z) \tag{8}$$

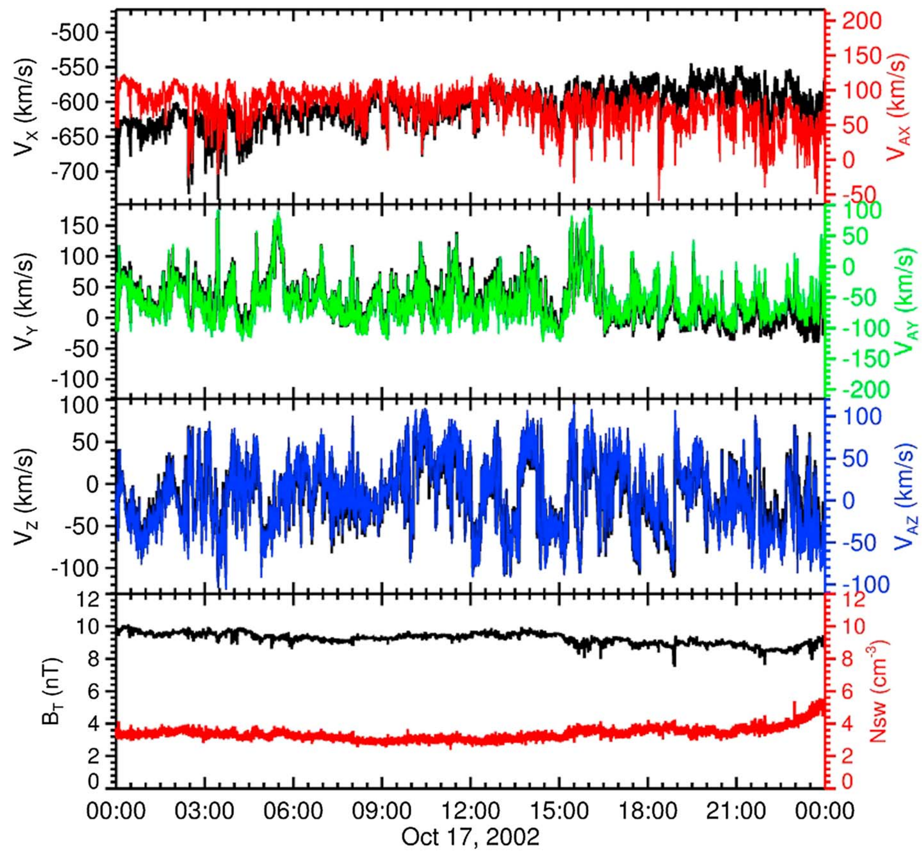

Figure 1. A long-interval large-amplitude Alfvén wave event on 17 October 2002. The first, second, and third panels show the solar wind velocity **V** and Alfvén speed $\mathbf{V}_A$, and the fourth panel gives the magnetic field strength and solar wind number density, B_T and N_{sw}, respectively. All the data with a temporal resolution of 3 s are from the Wind spacecraft. The magnetic field and solar wind velocity are in geocentric solar ecliptic (GSE) coordinates.

where γ_c is the correlation coefficient between all the components of band-passed plasma velocity fluctuation and Alfvén velocity fluctuation, $\sigma_{\delta\mathbf{V}}$ represents the standard deviation of all the components of band-passed plasma velocity fluctuation, and $\sigma_{\delta\mathbf{V}_A}$ represents the standard deviation of all the components of band-passed Alfvén velocity fluctuation. The terms with subscript i are just for the x, y, and$z$ components. From the calculation of E_{rr}, it is clear that E_{rr} is stricter than the parameter α (which is similar to Walén slope), Walén slope ($\gamma_c \times \frac{\sigma_{\delta V}}{\sigma_{\delta V_A}}$), and correlation coefficient γ_c. The closer the E_{rr} is to 0, the better Walén test is satisfied. For practice, $E_{rr} < 0.15$ is defined to represent a pure Alfvén wave. Compared to the results of previous studies (the Alfvénicity is less than 0.7, so E_{rr} is often greater than 0.3), our present threshold of 0.15 is stricter already than previous definitions.

3. Results

3.1. Long-Interval Alfvén Wave Event

Figure 1 shows the overall view of an large-amplitude Alfvén wave event on 17 October 2002 with a long interval of 1 day. This event is in the interaction region between two successive high-speed solar wind streams. The solar wind velocity **V** and Alfvén speed $\mathbf{V}_A$ correlate very well for the y and z components. For the x component, the V_x represents an overall deviation from V_{Ax}. It seems that the daily data set can be roughly divided into five intervals according to the relevancy of V_x and V_{Ax}: (1) 00:00–04:00 UT, V_x has a large downward deviation from V_{Ax}; (2) 04:00–09:00 UT, V_x has a less downward deviation from V_{Ax}; (3) 09:00–15:00 UT, V_x matches V_{Ax} very well; (4) 15:00–19:00 UT, V_x has a little upward deviation from V_{Ax}; and (5) 19:00–24:00 UT, V_x has a larger upward deviation from V_{Ax}. This indicates that the x component of the HT frame velocity varies

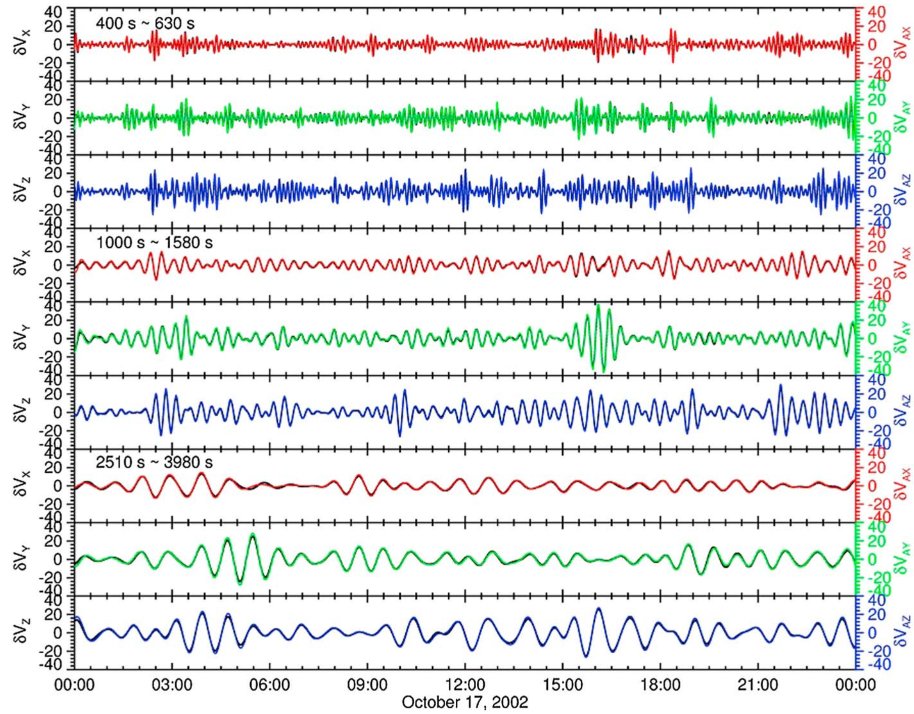

Figure 2. Three examples of the correlations between δV_i and δV_{Ai} from the selected filters (from top to bottom: 400 s–630 s, 1000 s–1580 s, 2510 s–3980 s) for Alfvén wave event on 17 October 2002 (red: *x* component; green: *y* component; blue: *z* component).

significantly during this event. Except for a gradual enhancement of solar wind number density (N_{sw}) after 22:00 UT, the magnitude of magnetic field (B_T) and N_{sw} are nearly stable for this event, with the standard derivations less than 5%.

For this daily data set, the filters are chosen from equation (6) to be 10 s–15 s, 15 s–25 s, 25 s–40 s, 40 s–60 s, 60 s–100 s, 100 s–160 s, 160 s–250 s, 250 s–400 s, 400 s–630 s, 630 s–1000 s, 1000 s–1580 s, 1580 s–2510 s, 2510 s–3980 s, 3980 s–6310 s, 6310 s–10,000 s, 10,000 s–15,850 s, 15,850 s–25,120 s. Figure 2 shows three examples of the comparisons of $\delta\mathbf{V}$ and $\delta\mathbf{V}_A$. $\delta\mathbf{V}$ and $\delta\mathbf{V}_A$ are the band-passed wave signals of $\mathbf{V}$ and $\mathbf{V}_A$, respectively. From top to bottom, every three panels show the results for the filters of 400 s–630 s, 1000 s–1580 s, and 2510 s–3980 s. It is clear that each component of $\delta\mathbf{V}$ and $\delta\mathbf{V}_A$ are correlated at a very high degree of perfection. Figure 3 gives the corresponding Walén tests for these three filtered wave signals. The correlation coefficients are all nearly 0.99, which is comparable to the Alfvén wave reported by *Wang et al.* [2012]. Note that this event has a much longer time interval (1 day, compared to less than 40 min).

Table 1 gives E_{rr}, the normalized cross helicity (σ_C) and the normalized residual energy (σ_R) of the wave signals from different filters for this event. For these 17 filtered wave signals, the E_{rr} are all less than 0.10, with the average value of 0.05. This further indicates that all the filtered wave fluctuations are nearly purely Alfvénic. The wave signal with period ranging from 100 s to 160 s has the highest degree of Alfvénicity, with E_{rr} of only 0.0377. The wave signal with period ranging from 15,850 s to 25,120 s has the lowest degree of Alfvénicity, with E_{rr} of 0.0803. As shown in the first panel of Figure 1, it seems that the HT frame for this event changes at a period of about 5 h (18,000 s), which belongs to the scope of last filter (15,850 s–25,120 s). As pointed out before, the effect of a varying HT frame can not be removed completely under this situation. Thus, the Alfvénicity of the wave signal with period ranging from 15,850 s to 25,120 s is the lowest. The results of σ_C is similar to that of E_{rr}, indicating E_{rr} can represent how well the Walén relation is satisfied as well. The σ_R is -0.127, which is also in agreement with previous studies [*Bavassano et al.*, 1998; *Bruno et al.*, 2007]. The σ_C for original data is only 0.826, much less than the average value for filtered data.

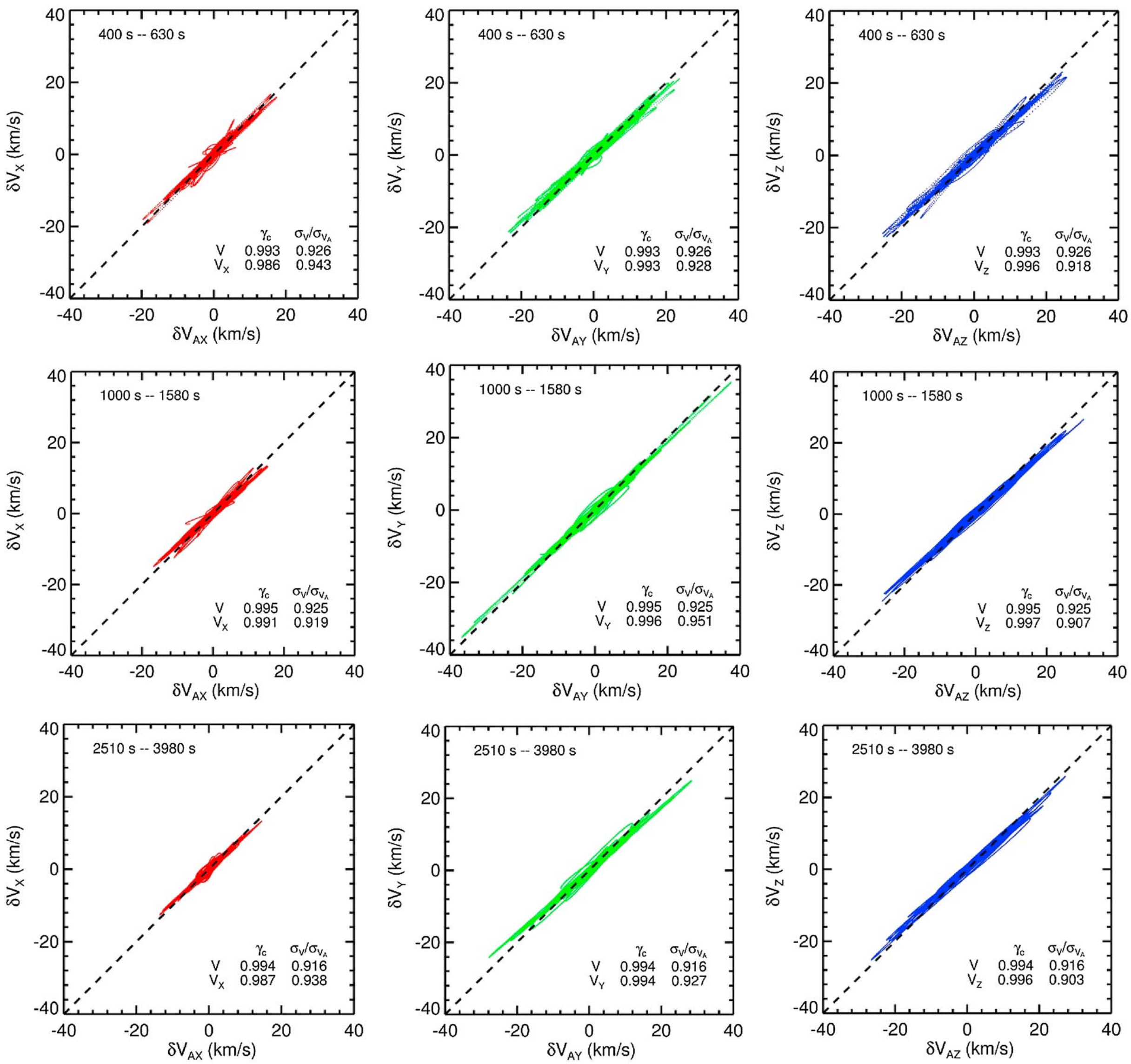

Figure 3. Results of Walén test for the three wave signals shown in Figure 2.

To validate our data analysis, the comparison of E_{rr} obtained from the three methods (denoted as method 1, method 2, and method 3) described by *Chao et al.* [2014] with our results is shown in Table 2. Method 1 and method 2 used equation (5) to calculate the Alfvénicity. The only difference is how to determine the HT frame. Method 1 minimized the average convection electric field,

$$D = \frac{1}{N}\sum_{i=1}^{N}\left|\left(\mathbf{V}^i - \mathbf{V}_{\mathrm{HT}}\right)\times\mathbf{B}^i\right|^2 \tag{9}$$

by solving

$$\partial D/\partial \mathbf{V}_{\mathrm{HT}} = 0 \tag{10}$$

Then, the HT frame velocity can be determined. Method 2 used the three geocentric solar ecliptic (GSE) components of the solar wind velocity $\mathbf{V}$ and the Alfvén velocity $\mathbf{V}_A$ to obtain the HT frame as follows:

$$\mathbf{V}_{\mathrm{HT}} = \frac{1}{N}\sum_{i=1}^{N}\left(\mathbf{V}_A^i - \mathbf{V}^i\right) \tag{11}$$

Method 3 used a sequence of data generated by taking the difference of two consecutive values of plasma and Alfvén velocities, respectively. For method 1 and method 2, the E_{rr} are 0.11 and 0.16, respectively.

Table 1. E_{rr}, σ_C (Normalized Cross Helicity), and σ_R (Normalized Residual Energy) of the Wave Signals From Different Filters for the Alfvén Wave Event on 17 October 2002

Filter	E_{rr}	σ_C	σ_R
10–15	0.0733	0.8084	−0.1061
15–25	0.0735	0.8984	−0.1114
25–40	0.0558	0.9446	−0.1061
40–60	0.0451	0.9655	−0.1073
60–100	0.0387	0.9739	−0.1064
100–160	0.0377	0.9777	−0.1104
160–250	0.0392	0.9807	−0.1157
250–400	0.0416	0.9806	−0.1243
400–630	0.0397	0.9817	−0.1245
630–1000	0.0418	0.9818	−0.1256
1000–1580	0.0398	0.9819	−0.1192
1580–2510	0.0361	0.9796	−0.1214
2510–3980	0.0430	0.9686	−0.1357
3980–6310	0.0436	0.9647	−0.1553
6310–10000	0.0505	0.9379	−0.1320
10000–15850	0.0706	0.8889	−0.1180
15850–25120	0.0803	0.8051	−0.2349
Average	0.0500	0.9424	−0.1267

The results obtained from the original data and from the 5-point smoothed data are quite the same. For method 3, the E_{rr} obtained from the 5-point smoothed data is 0.0468, which is much less than that from the original data. As previously shown in Table 1, the mean E_{rr} obtained by our method is 0.0500, which is at the same level of method 3 by using smoothed data and is much less than the results obtained by method 1 and method 2. It should be pointed out that the not shown correlation coefficients between V'_X and V'_{AX} for method 1 and method 2 are only 0.3 because of the varying HT frame.

Table 3 gives the properties of the wave signals from different filters for the Alfvén wave event on 17 October 2002. Alfvén waves observed in the solar wind are not necessarily periodic similar to a monochromatic wave. It is assumed that the Alfvén waves are broadband and propagate in a same direction for each filter. In general, the Alfvén waves are mostly propagating waves in interplanetary solar wind. We give the normal vector of wave propagating direction (**n**), the angle between the phase velocity direction of the Alfvén wave and the background magnetic field direction (θ_{Bn}), the degree of polarization (Dop = 1: completely polarized; Dop = 0: unpolarized; otherwise, partially polarized), and the ellipticity (1: circular polarization; 0: linear polarization, otherwise, elliptical polarization). The wave propagating direction is hard to determine accurately from the data of a single satellite. The minimum-variance direction obtained from the MVA analysis is assumed to be the wave propagating direction. As emphasized by *Wang et al.* [2012], the ratio of the intermediate to the minimum eigenvalue is an important indicator of the MVA accuracy. For our analysis, the mean value for these 17 wave signals is 3.3, which can confirm the credibility of our MVA results. Although it is not appropriate to take the average value to be the background state, such inaccurate background magnetic field can still be regarded as a reference direction in calculating θ_{Bn} here. The wave properties, such as the degree of polarization and the ellipticity, are obtained from the method introduced by *Fowler et al.* [1967].

Table 2. Comparison of E_{rr} Obtained From the Three Methods (Denoted as Method 1, Method 2, and Method 3) Detailed Described by *Chao et al.* [2014] With Our Results

	Original data	5-point smoothed data
Method 1	0.1055	0.1080
Method 2	0.1632	0.1660
Method 3	0.2895	0.0468
Our result	0.0500	

As shown in Table 3, all the wave signals propagate outward from the Sun. Except for the wave signal with the longest period, the other wave signals

Table 3. Properties of the Wave Signals From Different Filters for the Alfvén Wave Event on 17 October [a]

Filter	n	θ_{Bn}	Dop	Ellipticity
10–15	(−0.886, 0.458, −0.072)	170.3	0.11	0.03
15–25	(−0.879, 0.470, −0.078)	171.0	0.12	0.08
25–40	(−0.877, 0.471, −0.093)	170.8	0.12	0.02
40–60	(−0.858, 0.507, −0.079)	173.4	0.13	0.04
60–100	(−0.848, 0.521, −0.096)	173.9	0.16	0.12
100–160	(−0.858, 0.478, −0.188)	168.6	0.22	0.04
160–250	(−0.881, 0.447, −0.157)	168.1	0.19	0.08
250–400	(−0.869, 0.471, −0.151)	169.6	0.22	0.05
400–630	(−0.920, 0.373, −0.122)	164.6	0.16	0.11
630–1000	(−0.858, 0.510, −0.066)	173.7	0.28	0.27
1000–1580	(−0.907, 0.415, −0.070)	167.6	0.29	0.59
1580–2510	(−0.852, 0.523, 0.026)	173.3	0.28	0.05
2510–3980	(−0.906, 0.423, −0.035)	168.1	0.46	0.20
3980–6310	(−0.887, 0.454, 0.088)	167.7	0.51	0.03
6310–10000	(−0.962, 0.272, −0.007)	158.8	0.31	0.41
10000–15850	(−0.852, 0.516, −0.086)	173.8	0.52	0.44
15850–25120	(−0.350, 0.686, −0.638)	136.0	0.49	0.30

[a] n is the normal vector of the propagating direction. θ_{Bn} is the angel between the normal vector of propagating direction and the background magnetic field. Dop represents the degree of polarization (Dop = 1: completely polarized; Dop = 0: unpolarized; otherwise, partially polarized). Ellipticity is defined as the ratio of the minor and major axes of polarization ellipse (1: circular polarization; 0: linear polarization; otherwise, elliptical polarization).

propagate almost in a same direction, with a mean deviation of only 7°. The mean normal vector of the propagating direction is (-0.887, 0.455, -0.074), which is nearly antiparallel to the background magnetic field. The averaged θ_{Bn} is 170.4. Based on Dop, these wave signals can be divided into four groups: (1) Group 1 contains four filtered wave signals, with the period ranging from 10 s to 60 s. The mean Dop is 0.12; (2) Group 2 contains five filtered wave signals, with the period ranging from 60 s to 630 s. The mean Dop is 0.19; (3) Group 3 contains three filtered wave signals, with the period ranging from 630 s to 2510 s. The mean Dop is 0.28; (4) Group 4 contains five filtered wave signals, with the period ranging from 2510 s to 25,120 s. The mean Dop is 0.46. A clear trend is that the wave signal becomes more polarized gradually (increasing Dop) as the wave period increases. Meanwhile, the mean values of the ellipticity for these four groups are 0.04, 0.08, 0.30, and 0.28, respectively. The wave signal changes from a quasi-linear polarization to a more circular elliptical polarization.

3.2. Time-Frequency Distribution of Alfvénicity for Two Intervals of Solar Wind High-Speed Streams

Figure 4 shows the time-frequency distribution of the Alfvénicity for two long intervals of solar wind high-speed streams, (1) 25 January to 10 February 1995 and (2) 11 to 28 October 2002. Hourly data sets with 30 min running shift are used to obtain this contour plot. As described previously, a hourly data set is decomposed into 10 wave signals by different filters, with the frequency ranging from 1 mHz to 0.1 Hz. For these 10 filtered wave signals, only the situation that one of E_{rr} is less than 0.15 will be plotted. The green and blue regions represent large Alfvénicity. From this figure, we can easily find at what frequency the fluctuations are Alfvénic and their corresponding Alfvénicities.

As suspected by *Chao et al.* [2014], pure Alfvénic waves are frequently found at 1 AU in the solar wind during these two intervals. During the interval from 25 January to 10 February 1995, there occurs an isolated high-speed solar wind stream. The leading part is from 29 January 00:00 UT to 30 January 12:00 UT, and the trailing part is from 30 January 12:00 UT to 6 February 00:00 UT. The large Alfvénicities are most found in the trailing part, although it also exists in the leading part. During the interval from 11 to 28 October 2002, the high-speed streams are more complicated. There are three successive high-speed solar wind streams: (1) stream 1 starts from 14 October 00:00 UT, with V_x peaking at about 17 October 00:00 UT; (2) stream 2 starts from 18 October 12:00 UT and ends at 23 October 12:00 UT; (3) stream 3 is from 24 October 00:00 UT to 27 October 00:00 UT. Stream 2 moves faster than stream 1. It enters into the trailing part of stream 1 and interacts with stream 1. Similar to the previous interval, large Alfvénicities are more frequently found in the trailing part

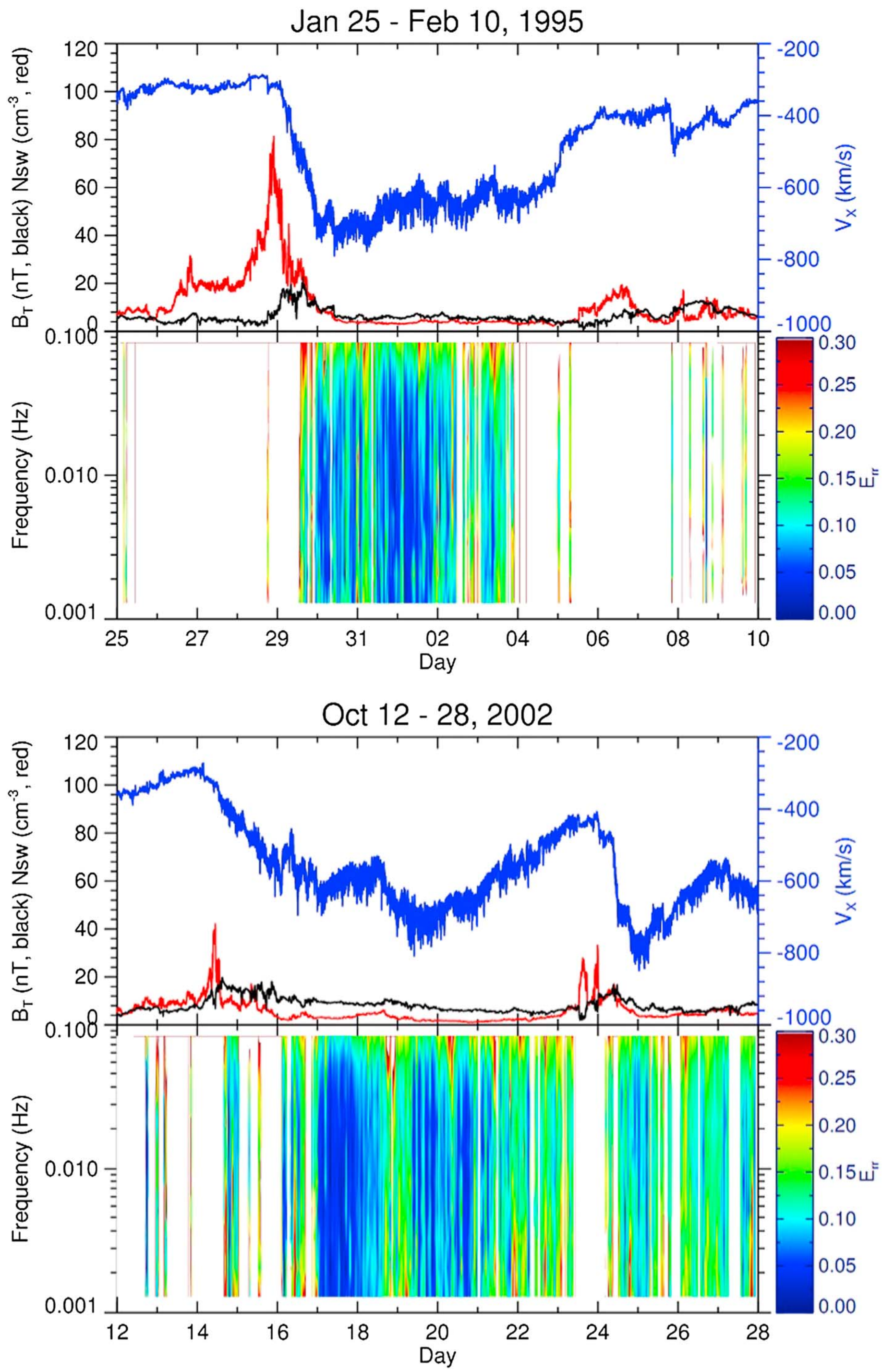

Figure 4. Time-frequency distribution of Alfvénicity for two intervals of solar wind high-speed streams. (top) 25 January to February 10 1995; (bottom) 11 to 28 October 2002. The first panel shows the magnitude of magnetic field (B_T), the number density of solar wind (N_{sw}), and the x component of solar wind velocity (V_x). The second panel gives the time-frequency distribution of E_{rr}.

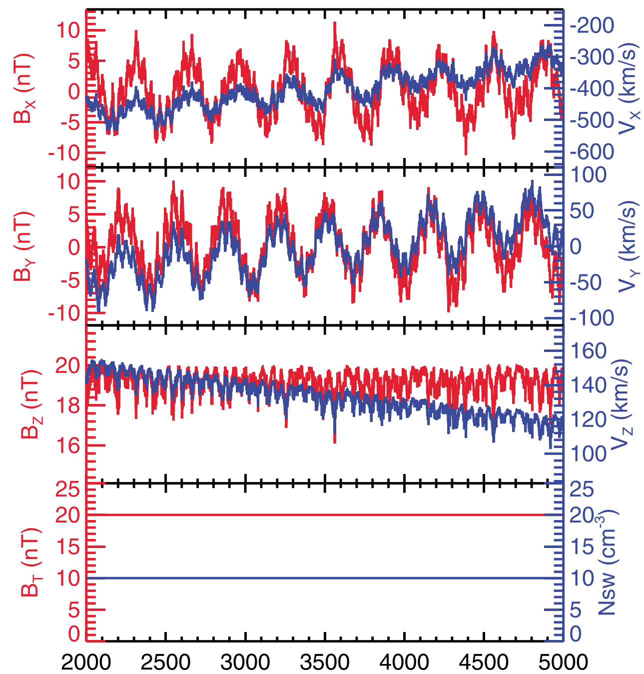

Figure 5. Simulated data of Alfvén waves with the temporal resolution of 1 s. The top three panels show the solar wind velocity **V** and the magnetic field **B**, and the bottom panel gives the magnetic field strength and solar wind number density, B_T and N_{sw}, respectively.

of high-speed solar wind stream than in the leading part. In particular, the largest Alfvénicities are found in the interaction region of stream 1 and stream 2. More detailed statistical study will be performed in the future.

4. Robustness Verification

To verify the robustness of the proposed technique, we applied it to simulated pure Alfvén waves with two separate frequencies and contaminated by pink colored noises in a varying solar wind stream. The HT frame is assumed to vary as follows:

$$\begin{cases} V_{\mathbf{HT}x} = -600 + t/18 \\ V_{\mathbf{HT}y} = -100 + t/36 \\ V_{\mathbf{HT}z} = 40 - t/90 \end{cases} \tag{12}$$

The simulated data are shown in Figure 5, and the details are given as follows:

$$\begin{cases} N_{\mathrm{SW}} = 10 \\ B_{\mathrm{T}} = 20 \\ B_{X1} = 5\sin(2\pi f_1 t);\ B_{X2} = 2\sin(2\pi f_2 t) \\ B_X = B_{X1} + B_{X2} + \mathrm{Pink\_Noise1} \\ B_{Y1} = 5\cos(2\pi f_1 t);\ B_{Y2} = 2\cos(2\pi f_2 t) \\ B_Y = B_{Y1} + B_{Y2} + \mathrm{Pink\_Noise2} \\ B_Z = \sqrt{{B_T}^2 - {B_X}^2 - {B_Y}^2} \\ V_X = V_{\mathbf{HT}x} + \frac{21.8122(B_{X1}+B_{X2})}{\sqrt{N_{\mathrm{SW}}}} + \mathrm{Pink\_Noise3} \\ V_Y = V_{\mathbf{HT}y} + \frac{21.8122(B_{Y1}+B_{Y2})}{\sqrt{N_{\mathrm{SW}}}} + \mathrm{Pink\_Noise4} \\ V_Z = V_{\mathbf{HT}z} + \frac{21.8122 B_Z}{\sqrt{N_{\mathrm{SW}}}} \end{cases} \tag{13}$$

Here f_1 = 1/320 Hz, and f_2 = 1/50 Hz. Pink_Noise 1 , Pink_Noise 2, Pink_Noise 3, and Pink_Noise 4 are pink colored noises generated by computer.

Table 4. E_{rr} of the Wave Signals From Different Filters for the Simulated Alfvén Waves

Filter	E_{rr}	Filter	E_{rr}
10–15	0.1682	100–160	0.1737
15–25	0.1667	160–250	0.1233
25–40	0.1456	250–400	0.0038
40–60	0.0023	400–630	0.1274
60–100	0.1292	630–1000	0.1603

We apply our method to this simulated data and calculate the E_{rr} for 10 frequency bands, which are listed in Table 4. It is clear that the E_{rr} of the wave signals from 40 s $\sim$ 60 s and 250 s $\sim$ 400 s filters are quite close to 0, indicating that the fluctuations in these two frequency bands are purely Alfvénic. This is consistent with our initializations that the frequencies of pure Alfvén waves are 1/50 Hz and 1/320 Hz. If the conventional Walén test is applied to this simulated data, the E_{rr} will be 0.7351, indicating that the fluctuations are not pure Alfvénic. Thus, our analysis technique is more robust than the conventional Walén test and can perform well for pure Alfvén waves with separated narrow frequency bands and contaminated by pink colored noises in a varying solar wind stream.

5. Summary

In conventional analysis of interplanetary Alfvén waves, an accurately determined HT frame or background magnetic field is required to check the validity of the Walén relation. Usually, the HT frame velocity is assumed to be stable during the time interval concerned and is obtained from the MVA technique. However, such an averaged HT frame may not be adequate for some dynamic solar wind structures. Using a window of duration of T with a Δt shift is indeed a possible approach to determine a varying HT frame. However, the choice of T is artificial. Meanwhile, the MVA technique depends on the data points sampled. Sometimes, in practice, the result is quite sensitive to T, and the relative difference is unacceptable. Thus, such an attempt to determine a varying HT frame for the Walén test is rarely reported. The background magnetic field is not an observable quantity or easily determined. It is also not always appropriate to take the average value of the magnetic field to be the background state. Thus, *Gosling et al.* [2009] suggested that the conclusions derived from the analyses by assuming the fluctuations in all field components are relative to average values need to be reexamined.

Many previous studies reveal that the strength of solar wind Alfvénicity near 1 AU is only 0.7 or less. However, *Wang et al.* [2012] presented a clear case of pure large-amplitude Alfvén wave near 1 AU, with the Alfvénicity nearly equal to 1. Recently, *Gosling et al.* [2009] and *Chao et al.* [2014] proposed a method, which is independent of HT frame, to check the Walén relation, and which can predict Alfvénic fluctuations well. *Chao et al.* [2014] then suspected that pure Alfvénic waves should be found frequently near 1 AU. Nevertheless, very little attentions have been paid to the frequency properties of interplanetary Alfvén waves.

In order to reduce the uncertainty introduced by determining the HT frame and background magnetic field, a new approach is applied to do the Walén test for indentifying the interplanetary large-amplitude Alfvén waves in this study. Our approach is independent of the HT frame and background magnetic field. Instead of the original data sets, the band-pass filtered signals of plasma velocity and magnetic field observations are used here. The robustness of this technique is also verified. Compared to the conventional Walén test, this new approach can perform well for pure Alfvén waves with separated narrow frequency bands and contaminated by pink colored noises in a varying solar wind stream. Moreover, our new technique can be applied to identify narrow band or nearly monochromatic Alfvén waves with a bump in the field power spectra shown by *Wang et al.* [2015]. In this regard, this new technique will improve the understanding of interplanetary Alfvén waves.

Furthermore, more extensive properties of Alfvén waves in frequency domain can be obtained with our method. These properties have rarely been discussed before. We applied our analysis approach to two long intervals of solar wind high-speed streams, finding that nearly pure large-amplitude Alfvén waves are frequently found near 1 AU during these two intervals.

Acknowledgments
We thank the CDAWEB (http://cdaweb.gsfc.nasa.gov/istp_public) for access to the data from Wind Mission. We also would like to thank Shuo Yao and Lei Yang for frequent discussion on the Walén test for Alfvén waves in interplanetary space. This work was supported by 973 program 2012CB825602, NNSFC grants 41574169, 41204118, 41231067, 41174142, and 41174149. H. Li was also supported by Youth Innovation Promotion Association of the Chinese Academy of Sciences and in part by the Specialized Research Fund for State Key Laboratories of China.

References

Alazraki, G., and P. Couturie (1971), Solar wind acceleration caused by gradient of Alfven wave pressure, *Astron. Astrophys.*, *13*(3), 380–389.
Alfvén, H. (1942), Existence of electromagnetic-hydrodynamic waves, *Nature*, *150*(3805), 405–406, doi:10.1038/150405d0.
Barnes, A., and J. V. Hollweg (1974), Large-amplitude hydromagnetic waves, *J. Geophys. Res.*, *79*(16), 2302–2318, doi:10.1029/JA079i016p02302.

Bavassano, B., E. Pietropaolo, and R. Bruno (1998), Cross-helicity and residual energy in solar wind turbulence: Radial evolution and latitudinal dependence in the region from 1 to 5 AU, *J. Geophys. Res.*, *103*(A4), 6521–6529.

Belcher, J. W., and L. Davis (1971), Large-amplitude Alfvén waves in interplanetary medium, 2, *J. Geophys. Res.*, *76*(16), 3534–3563, doi:10.1029/JA076i016p03534.

Belcher, J. W., L. Davis, and E. J. Smith (1969), Large-amplitude Alfvén waves in interplanetary medium mariner 5, *J. Geophys. Res.*, *74*(9), 2302, doi:10.1029/JA074i009p02302.

Bruno, R., and V. Carbone (2013), The solar wind as a turbulence laboratory, *Living Rev. Solar Phys.*, *10*, 2, doi:10.12942/lrsp-2013-2.

Bruno, R., B. Bavassano, and U. Villante (1985), Evidence for long period Alfvén waves in the inner solar system, *J. Geophys. Res.*, *90*, 4373–4377.

Bruno, R., B. Bavassano, R. D'Amicis, V. Carbone, L. Sorroso-Valvo, and E. Pietropaolo (2006), On the radial evolution of Alfvénic turbulence in the solar wind, *Space. Sci. Rev.*, *122*, 321–328, doi:10.1007/s11214-006-5232-8.

Bruno, R., R. D'Amicis, B. Bavassano, V. Carbone, and L. Sorriso-Valvo (2007), Magnetically dominated structures as an important component of the solar wind turbulence, *Ann. Geophys.*, *25*, 1913–1927.

Burlaga, L. F. (1971a), Nature and origin of directional discontinuities in solar wind, *J. Geophys. Res.*, *76*(19), 4360–4365, doi:10.1029/JA076i019p04360.

Burlaga, L. F. (1971b), Hydromagnetic waves and discontinuities in solar wind, *Space Sci. Rev.*, *12*(5), 600–657.

Chao, J. K., W. C. Hsieh, L. Yang, and L. C. Lee (2014), Walen Test and De Hoffmann-Teller Frame of interplanetary large-amplitude Alfvén waves, *Astrophys. J.*, *786*, 149, doi:10.1088/0004-637X/786/2/149.

Coleman, P. J. (1967), Wave-like phenomena in interplanetary plasma: Mariner 2, *Planet. Space Sci.*, *15*(6), 953–973, doi:10.1016/0032-0633(67)90166-3.

Coleman, P. J. (1968), Turbulence, viscosity, and dissipation in the solar-wind plasma, *Astrophys. J.*, *153*, 371–388.

de Hoffmann, F., and E. Teller (1950), Magneto-hydrodynamic shocks, *Phys. Rev.*, *80*, 692–703.

Dobrowolny, M., A. Mangeney, and P. L. Veltri (1980), Properties of magnetohydrodynamic turbulence in the solar wind, in *Solar and Interplanetary Dynamics*, pp. 143–146, Springer, Netherlands.

Fowler, R. A., B. J. Kotick, and R. D. Elliott (1967), Polarization analysis of a natural and artificially induced geomagnetic micropulsations, *J. Geophys. Res.*, *72*(11), 2871–2883, doi:10.1019/JZ072i011p02871.

Gosling, J. T., D. J. McComas, D. A. Roberts, and R. M. Skoug (2009), A one-sided aspect of Alfvenic fluctuations in the solar wind, *Astrophys. J. Lett.*, *695*(2), L213–L216.

Gosling, J. T., W. L. Teh, and S. Eriksson (2010), A torsional Alfven wave embedded within a small magnetic flux rope in the solar wind, *Astrophys. J. Lett.*, *719*(1), L36–L40.

Gosling, J. T., H. Tian, and T. D. Phan (2011), Pulsed Alfven waves in the solar wind, *Astrophys. J. Lett.*, *737*(2), doi:10.1088/2041-8205/737/2/L35.

He, J., Z. Pei, L. Wang, C. Tu, E. Marsch, L. Zhang, and C. Salem (2015), Sunward propagating Alfvén waves in association with sunward drifting proton beams in the solar wind, *Astrophys. J.*, *805*(2), 176, doi:10.1088/0004-637X/805/2/176.

Hudson, P. D. (1971), Rotational discontinuities in an anisotropic plasma, *Planet. Space Sci.*, *19*(12), 1693, doi:10.1016/0032-0633(71)90129-2.

Lepping, R. P., et al. (1995), The wind magnetic field investigation, *Space Sci. Rev.*, *71*(1–4), 207–229.

Lichtenstein, B. R., and C. P. Sonett (1979), Angle between the average inter-planetary magnetic-field and the propagation direction of plane large-amplitude alfven waves, *Geophys. Res. Lett.*, *6*(9), 713–716.

Lin, R. P., et al. (1995), A three-dimensional plasma and energetic particle investigation for the Wind spacecraft, *Space Sci. Rev.*, *71*(1–4), 125–153.

Marsch, E., and C. Y. Tu (1990), On the radial evolution of MHD turbulence in the inner heliosphere, *J. Geophys. Res.*, *95*, 8211–8229.

Matthaeus, W. H., M. L. Goldstein, and D. A. Roberts (1990), Evidence for the presence of quasi-two-dimensional nearly incompressible fluctuations in the solar wind, *J. Geophys. Res*, *95*, 20,673–20,683.

Mavromichalaki, H., et al. (1988), Relatively stable, large-amplitude Alfvénic waves seen at 2.5 and 5.0 AU, *Sol. Phys.*, *116*, 377–390.

McIntosh, S. W., et al. (2011), Alfvénic waves with sufficient energy to power the quiet solar corona and fast solar wind, *Nature*, *475*(7357), 477–480, doi:10.1038/nature10235.

Neugebauer, M. (2004), Anisotropy and Alfvénicity of hourly fluctuations in the fast polar solar wind, *J. Geophys. Res.*, *109*, A02101, doi:10.1029/2003JA009947.

Neugebauer, M. (2006), Comment on the abundances of rotational and tangential discontinuities in the solar wind, *J. Geophys. Res.*, *111*, A04103, doi:10.1029/2005JA011497.

Neugebauer, M., D. R. Clay, B. E. Goldstein, B. T. Tsurutani, and R. D. Zwickl (1984), A reexamination of rotational and tangential discontinuities in the solar wind, *J. Geophys. Res.*, *89*(A7), 5395–5408.

Paschmann, G., S. Haaland, B. Sonnerup, and T. Knetter (2013), Discontinuities and Alfvenic fluctuations in the solar wind, *Ann. Geophys.*, *31*(5), 871–887, doi:10.5194/angeo-31-871-2013.

Podesta, J., and A. Bhattacharjee (2010), Theory of incompressible magnetohydrodynamic turbulence with scale-dependent alignment and cross-helicity, *Astrophys. J.*, *718*(2), 1151.

Podesta, J., and J. Borovsky (2010), Scale invariance of normalized cross-helicity throughout the inertial range of solar wind turbulence, *Phys. Plasmas.*, *17*(11), 112905.

Riley, P., C. P. Sonett, B. T. Tsurutani, A. Balogh, R. J. Forsyth, and G. W. Hoogeveen (1996), Properties of arc-polarized Alfven waves in the ecliptic plane: Ulysses observations, *J. Geophys. Res.*, *101*(A9), 19,987–19,993, doi:10.1029/96ja01743.

Scudder, J. D., P. A. Puhl-Quinn, F. S. Mozer, K. W. Ogilvie, and C. T. Russell (1999), Generalized Walen tests through Alfven waves and rotational discontinuities using electron flow velocities, *J. Geophys. Res.*, *104*(A9), 19,817–19,833, doi:10.1029/1999ja900146.

Sonnerup, B. U. Ö., and L. J. Cahill Jr. (1967), Magnetopause structure and attitude from Explorer 12 observations, *J. Geophys. Res.*, *72*(1), 171–183, doi:10.1029/JZ072i001p00171.

Tsurutani, B. T., and W. D. Gonzalez (1987), The cause of High Intensity Long-Duration Continuous AE Activity (HILDCAAs): Interplanetary Alfvén wave trains, *Planet. Space Sci.*, *35*, 405–412.

Tu, C. Y., and E. Marsch (1993), A model of solar wind fluctuations with two components: Alfvén waves and convective structures, *J. Geophys. Res.*, *98*, 1257–1276.

Tu, C. Y., and E. Marsch (1995), MHD structures, waves and turbulence in the solar wind: Observations and theories, *Space Sci. Rev.*, *73*, 1–210.

Tu, C. Y., E. Marsch, and H. Rosenbauer (1990), The dependence of MHD turbulence spectra on the inner solar wind stream structure near solar minimum, *Geophys. Res. Lett.*, *17*, 283–286.

Unti, T. W. J., and M. Neugebauer (1968), Alfvén waves in the solar wind, *Phys. Fluids*, *11*, 563.

Völk, H. J. (1975), Microstructure of solar-wind, *Space Sci. Rev.*, *17*(2–4), 255–276.
Walén, C. (1944), On the theory of sunspots, *Ark. Fys.*, *30*, 1.
Wang, X., J. S. He, C. Y. Tu, E. Marsch, L. Zhang, and J. K. Chao (2012), Large-amplitude Alfvén wave in interplanetary space: The Wind spacecraft observations, *Astrophys J.*, *746*, 147, doi:10.1088/0004-637X/746/2/147.
Wang, X., C. Tu, L. Wang, J. He, and E. Marsch (2015), The upstream-propagating Alfvénic fluctuations with power law spectra in the upstream region of the Earth's bow shock, *Geophys. Res. Lett.*, *42*, 3654–3661, doi:10.1002/2015GL063893.
Wentzel, D. G. (1974), Coronal heating by Alfven Waves, *Sol. Phys.*, *39*(1), 129–140.
Wicks, R. T., D. A. Roberts, A. Mallet, A. A. Schekochihin, T. S. Horbury, and C. H. Chen (2013), Correlations at large scales and the onset of turbulence in the fast solar wind, *Astrophys J.*, *778*, 177, doi:10.1088/0004-637X/778/2/177.
Yang, L., and J. K. Chao (2013), Alfvén waves in the solar wind, *Chin. J. Space Sci.*, *33*(4), 353–373.